On the Application of Under-Decimated Filter Banks

Y.-P. Lin and P. P. Vaidyanathan

California Institute of Technology

Maximally decimated filter banks have been extensively studied in the past. A filter bank is said to be under-decimated if the number of channels is more than the decimation ratio in the subbands. A maximally decimated filter bank is well known for its application in subband coding. Another application of maximally decimated filter banks is in block filtering. Convolution through block filtering has the advantages that parallelism is increased and data are processed at a lower rate. However, the computational complexity is comparable to that of direct convolution. More recently, another type of filter bank convolver has been developed. In this scheme, the convolution is performed in the subbands. Quantization and bit allocation of subband signals are based on signal variance, as in subband coding. Consequently, for a fixed rate, the result of convolution is more accurate than is direct convolution. This type of filter bank convolver also enjoys the advantages of block filtering, parallelism, and a lower working rate. Nevertheless, like block filtering, there is no computational saving.

In this article, under-decimated systems are introduced to solve the problem. The new system is decimated only by half the number of channels. Two types of filter banks can be used in the under-decimated system: the discrete Fourier transform (DFT) filter banks and the cosine modulated filter banks. They are well known for their low complexity. In both cases, the system is approximately alias free, and the overall response is equivalent to a tunable multilevel filter. Properties of the DFT filter banks and the cosine modulated filter banks can be exploited to simultaneously achieve parallelism, computational saving, and a lower working rate. Furthermore, for both systems, the implementation cost of the analysis or synthesis bank is comparable to that of one prototype filter plus some low-complexity modulation matrices. The individual analysis and synthesis filters have complex coefficients in the DFT filter banks but have real coefficients in the cosine modulated filter banks.

I. Introduction

The M channel maximally decimated filter bank shown in Fig. 1 has been studied extensively in [1–8]. A filter bank is said to be under-decimated if the number of channels is more than the decimation ratio in the subbands. When the system in Fig. 1 is alias free, it is a linear time invariant system with transfer function $T(z)$, as indicated in Fig. 1. In the following discussion, $T(z)$ will be called the distortion function, or the overall response.

A maximally decimated filter bank is well known for its application in subband coding. Another application of maximally decimated filter banks is in block filtering [9]. Convolution through block

filtering has the advantages that parallelism is increased and data are processed at a lower rate. However, the computational complexity is comparable to that in direct convolution. In [10], filter banks are used to map long convolutions into smaller ones in the subbands. Computations are then performed in parallel at a lower rate.
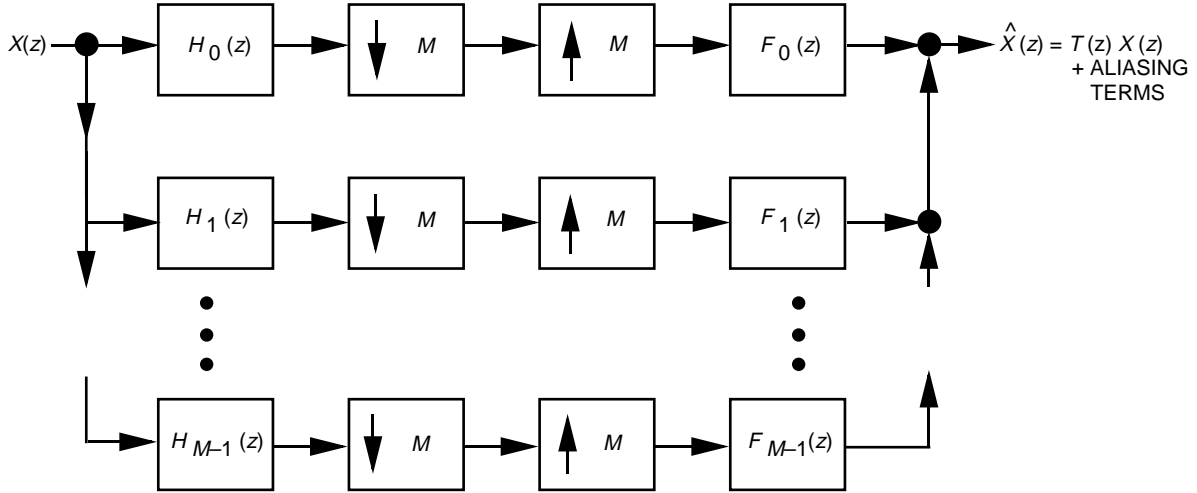

Fig. 1. The *M*–channel maximally decimated filter bank.

More recently [8], another type of filter bank convolver has been developed. In this scheme, the convolution is performed in the subbands. Quantization and bit allocation of subband signals are based on signal variance as in subband coding. Consequently, for a fixed rate, the result of convolution is more accurate than is direct convolution. This type of filter bank convolver also enjoys the advantages of block filtering, parallelism, and a lower working rate. Nevertheless, like block filtering, there is no computational saving.

In this article, under-decimated systems are introduced to solve the problem. Figure 2 shows the setup of the under-decimated system; it has $2M$ channels but is decimated only by M. Two types of filter banks can be used in the under-decimated system: the discrete Fourier transform (DFT) filter banks and the cosine modulated filter banks. They are recognized for their low complexity. In both cases, the system is approximately alias free and the overall response $T(z)$ is equivalent to a tunable multilevel filter. Properties of the DFT filter banks and the cosine modulated filter banks can be exploited to simultaneously achieve parallelism, computational saving, and a lower working rate. Furthermore, for both systems, the implementation cost of the analysis bank or the synthesis bank is comparable to that of one prototype filter plus some low complexity modulation matrices. The individual analysis and synthesis filters have complex coefficients in the DFT filter banks but have real coefficients in the cosine modulated filter banks.

This work is organized as follows: Section II is devoted to the construction of the new $2M$-channel under-decimated DFT filter bank. Suppression of alias error due to decimation in the subbands is elaborated, and implementation and complexity of this DFT filter bank are discussed therein. The new $2M$-channel cosine modulated filter bank is discussed in a similar manner in Section III. In the cosine modulated system, filters are real-coefficient and hence have positive and negative spectral occupancy. As a result, alias error in this case is more complicated than in DFT filter banks and requires careful treatment. Also in Section III, we study different types of spectral configuration for the under-decimated cosine modulated filter banks. Design examples are given in Section IV.

In this article, the following conventions are used:

(1) Bold faced lower-case letters are used to represent vectors, and bold faced upper-case letters are used to represent matrices.

(2) The notations $\mathbf{A}^T$, $\mathbf{A}^*$, and $\mathbf{A}^\dagger$ represent the transpose, conjugate, and transpose conjugate of $\mathbf{A}$, respectively. The "tilde" notation is defined as follows: $\widetilde{\mathbf{A}}(z) = \mathbf{A}^\dagger(1/z^*)$.

(3) Matrix $\mathbf{I}_k$ denotes a $k \times k$ identity matrix, and $\mathbf{J}_k$ denotes a $k \times k$ reversal matrix with

$$\mathbf{J}_k = \begin{pmatrix} 0 & \cdots & 0 & 1 \\ 0 & \cdots & 1 & 0 \\ \vdots & & \vdots & \vdots \\ 1 & \cdots & 0 & 0 \end{pmatrix}$$

(4) The delay chain $\mathbf{e}_k(z)$ is the vector $\mathbf{e}_k(z) = \begin{bmatrix} 1 & z^{-1} \cdots z^{-(k-1)} \end{bmatrix}^T$.

(5) The unit pulse, denoted as $\delta(n)$, is defined according to

$$\delta(n) = \begin{cases} 1 & \text{n} = 0, \\ 0 & \text{otherwise} \end{cases}$$

(6) The value of the function $\lfloor x \rfloor$ is the largest integer less or equal to x.

(7) The $2M \times 2M$ DFT matrix, $\mathbf{W}$, is defined such that $[\mathbf{W}]_{mn} = W^{mn}$. The quantity W is given by $W = e^{-j\pi/M}$, where $j = \sqrt{-1}$.

(8) A filter $H(z)$ is called a Nyquist (M) filter if its impulse response $h(n)$ satisfies $h(Mn) = c\delta(n)$, for some constant c.
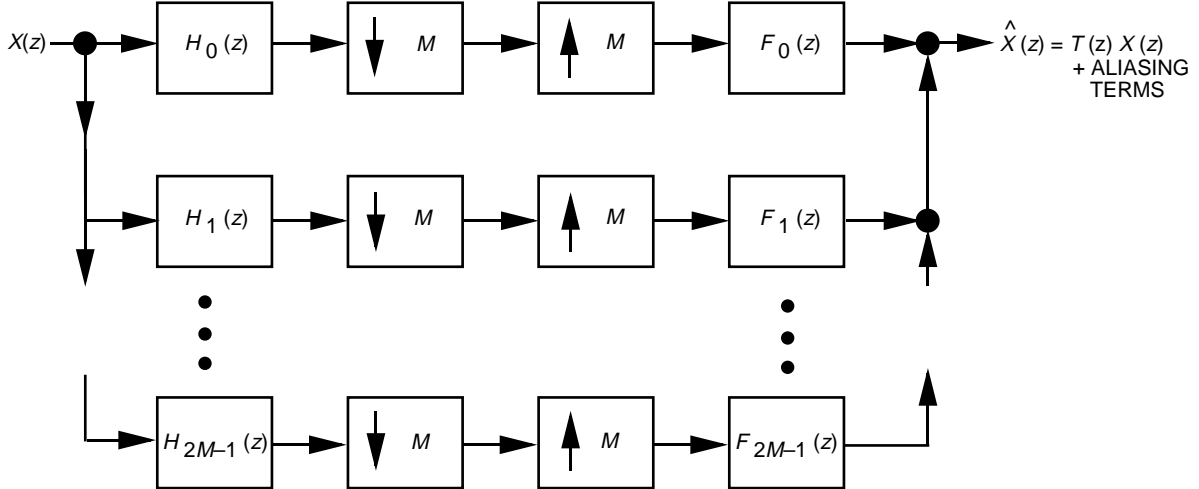

Fig. 2.   A 2*M*–channel under-decimated filter bank.

II. DFT Filter Banks and Their Application in Tunable Multilevel Filtering

The system in Fig. 2 is called a DFT filter bank if the analysis filters are shifted versions of the same prototype. The same holds for the synthesis bank. The prototype of the analysis bank and the prototype

of the synthesis bank need not be the same. To be more specific, let $P_0(z)$ be the prototype filter of the analysis bank and $Q_0(z)$ be the prototype filter of the synthesis bank. The filters $P_k(z)$ and $Q_k(z)$, $k = 1, 2, \cdots, 2M - 1$, are, respectively, the shifted versions of $P_0(z)$ and $Q_0(z)$.

$$P_k(z) = P_0(zW^k), \qquad Q_k(z) = Q_0(zW^k), \qquad k = -M, -M+1, \cdots, M-1$$

Notice that unit circle $P_k(z)$ is only a shift of $P_0(z)$ by $k\pi/M$, since $P_k(e^{j\omega}) = P_0(e^{j(\omega - k\pi/M)})$. Figure 3 shows this relationship. The analysis filters and synthesis filters of the DFT filter bank have the following form:

$$H_k(z) = a_k P_0(zW^k), \qquad \text{and} \qquad F_k(z) = a_k^* Q_0(zW^k), \quad W = e^{-j\pi/M} \tag{1}$$
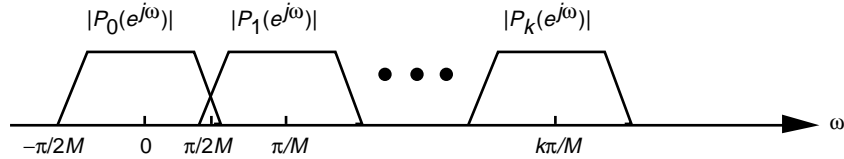

Fig. 3. Magnitude responses of $P_k(z)$.

(The definition of a DFT filter bank here is slightly different from the conventional DFT filter banks [7].) It follows that $H_k(e^{j\omega})$ is just a shift of $P_0(e^{j\omega})$ by $k\pi/M$ except for a scalar. The same holds for the synthesis filters.

We now show that with proper design of the two prototypes, this DFT filter is approximately alias free and the overall response is equivalent to a tunable multilevel filter. Moreover, the overall response can be a real-coefficient linear-phase filter as desired. Efficient implementation of the DFT filter bank will also be discussed.

A. Suppression of Aliasing Error

Consider the under-decimated system in Fig. 2, a $2M$-channel filter bank with decimation ratio M. The suppression of aliasing error due to downsampling in the subbands can be explained pictorially. Take the first subband as an example. Because of decimation followed by expansion, there will be $M-1$ image copies of $H_0(z)$, as shown in Fig. 4. We can see from Fig. 4 that these image copies will be suppressed if both $H_0(z)$ and $F_0(z)$ have stop-band edges less than π/M. When the spectral supports of $F_0(z)$ and the image copy of $H_0(z)$ do not overlap, the aliasing error will be suppressed to the level of the stop-band attenuation of $H_0(z)$ or $F_0(z)$, which is equivalent to the stop-band attenuation of $P_0(z)$ or $Q_0(z)$. In the other subbands, the same reasoning for aliasing suppression applies.

We now present the mathematical counterpart of the above discussion. The output $\widehat{X}(z)$ is related to the input $X(z)$ by

$$\widehat{X}(z) = \sum_{i=0}^{M-1} A_i(z) X(zW^{2i}) \tag{2}$$
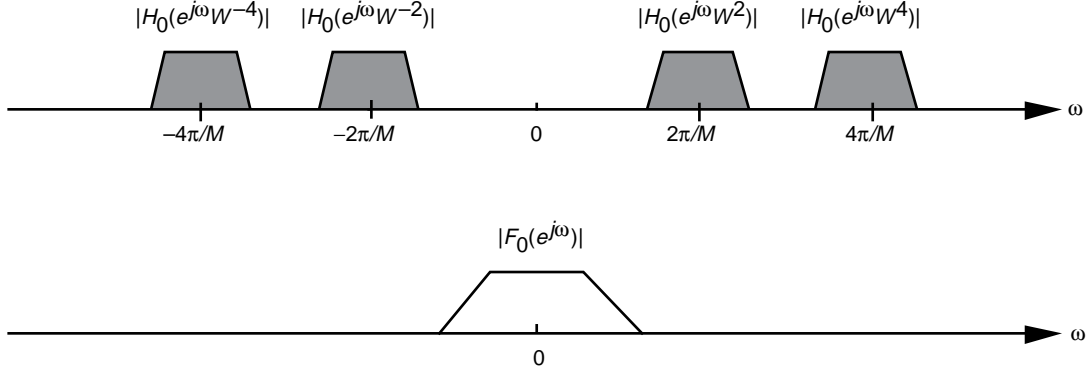
The alias transfer function, $A_i(z)$, is defined as

Fig. 4. Image copies of H_0 (z) due to decimation followed by expansion and the spectral support of F_0 (z).

$$A_i(z) = \frac{1}{M} \sum_{k=0}^{2M-1} H_k(zW^{2i})F_k(z) \tag{3}$$

The system in Fig. 2 is alias free if $A_i(z) = 0$ for $i = 1, 2, \cdots, M-1$. With analysis filters and synthesis filters chosen as in Eq. (1), $A_i(z)$ can be written as

$$A_i(z) = \frac{1}{M} \sum_{k=0}^{2M-1} |a_k|^2 P_0(zW^{2i+k})Q_0(zW^k) \tag{4}$$

Assume the nonadjacent bands of $P_0(z)$ and $Q_0(z)$ do not overlap, i.e.,

$$P_0(e^{j\omega}W^{2i})Q_0(e^{j\omega}) \approx 0, \quad i = 1, \cdots, M-1 \tag{5}$$

This assumption is reasonable if $P_0(z)$ and $Q_0(z)$ have stop-band edges less than π/M and large enough stop-band attenuation. Equation (5) gives us

$$H_k(zW^{2i})F_k(z) \approx 0, \quad k = 0, 1, \cdots, 2M-1, \quad i = 1, 2, \cdots, M-1$$

which implies $A_i(z) \approx 0, i \neq 0$. We conclude that the DFT filter bank is almost alias free. Also notice that the degree of alias suppression improves with the stop-band attenuation of the two prototypes.

B. The Overall Response of the DFT Filter Bank

For a $2M$-channel system decimated by M as shown in Fig. 2, the distortion function $T(z)$ can be expressed as [7]

$$T(z) = \frac{1}{M} \sum_{k=0}^{2M-1} H_k(z)F_k(z) \tag{6}$$

Let $R_0(z) = P_0(z)Q_0(z)$. Substitute the expression of $H_k(z)$ and $F_k(z)$ in Eq. (1); then

$$T(e^{j\omega}) = \frac{1}{M} \sum_{k=0}^{2M-1} |a_k|^2 R_0(e^{j(\omega-k\pi/M)}) \tag{7}$$

When $R_0(z)$ is a Nyquist $(2M)$ filter, it can be shown the addition of $|a_k|^2 R_0(e^{j(\omega - k\pi/M)})$ in Eq. (7) will not result in any bumps or dips in the response of $T(z)$ because of the Nyquist property of $R_0(z)$. The definition of a Nyquist filter is given in Section I. A detailed explanation can be found in [7].

With Eq. (7), we can plot a typical magnitude response of $T(z)$, as in Fig. 5, which shows that the overall response is equivalent to a multilevel filter. Since the value of a_k can be chosen freely, $T(z)$ is actually a tunable multilevel filter. In particular, we can get lowpass filters with stop-band edges adjustable in integer multiples of π/M.
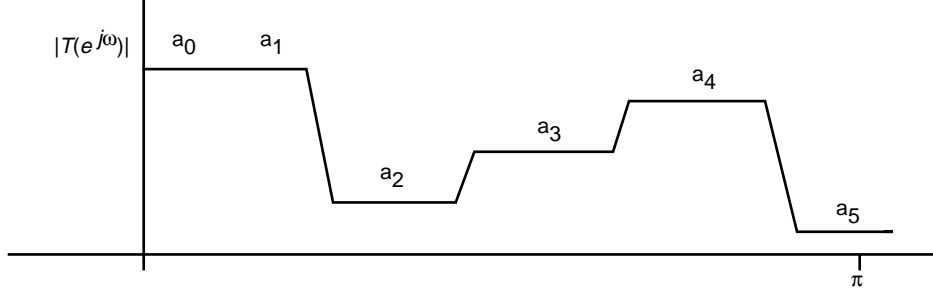

Fig. 5. A typical magnitude response of *T(z)*, a multilevel filter.

Remarks:

(1) If $R_0(z)$ is a real-coefficient filter and we choose $a_k = a_{2M-k}$ to be some real number, $k = 1, 2, \cdots, M$, it can be verified that the resulting $T(z)$ is also real-coefficient.

(2) Let $R_0(z)$ be linear phase with order N_r, a multiple of M. In this case, $R_0(zW^k)$ is linear phase. By Eq. (7), this implies that $T(z)$ has linear phase.

Summarizing, we have shown that if $R_0(z)$ is Nyquist $(2M)$ and Eq. (5) is valid, the DFT filter in Fig. 2 is nearly alias free and the overall response is equivalent to a tunable multilevel filter.

C. Implementation of the DFT Filter Bank

There exists an efficient implementation for the DFT filter bank. To see this, express the prototype $P_0(z)$ in polyphase representation, i.e.,

$$P_0(z) = \sum_{i=0}^{2M-1} E_i(z^{2M}) z^{-i} \tag{8}$$

where $E_i(z)$ is the ith type 1 polyphase component of $P_0(z)$ [7]. The analysis filters can be rewritten as

$$H_k(z) = a_k P_0(zW^k) = a_k \sum_{i=0}^{2M-1} E_i(z^{2M}) W^{-ki} z^{-i}, \quad k = 0, 1, \cdots, 2M-1 \tag{9}$$

Let

$$\mathbf{h}(z) = [H_0(z) \ H_1(z) \cdots \ H_{2M-1}(z)]^T \tag{10}$$

The matrix representation of Eq. (9) is

$$\mathbf{h}(z) = \begin{pmatrix} a_0 & 0 & \cdots & 0 \\ 0 & a_1 & \cdots & 0 \\ \vdots & \vdots & \ddots & \vdots \\ 0 & 0 & \cdots & a_{2M-1} \end{pmatrix} \mathbf{W}^* \begin{pmatrix} E_0(z^{2M}) & 0 & \cdots & 0 \\ 0 & E_1(z^{2M}) & \cdots & 0 \\ \vdots & \vdots & \ddots & \vdots \\ 0 & 0 & \cdots & E_{2M-1}(z^{2M}) \end{pmatrix} \mathbf{e}_{2M}(z) \qquad (11)$$

Observing Eq. (11), we can draw the polyphase implementation of the analysis bank as in Fig. 6. The implementation cost is that of the prototype filter $P_0(z)$ plus a DFT matrix. The same holds for the synthesis bank. The computational complexity of the analysis bank is comparable to that of the analysis prototype filter plus one DFT matrix. Notice that all the computations involved in the filter bank are performed after the M-fold decimators; lower rate and lower complexity are achieved at the same time.
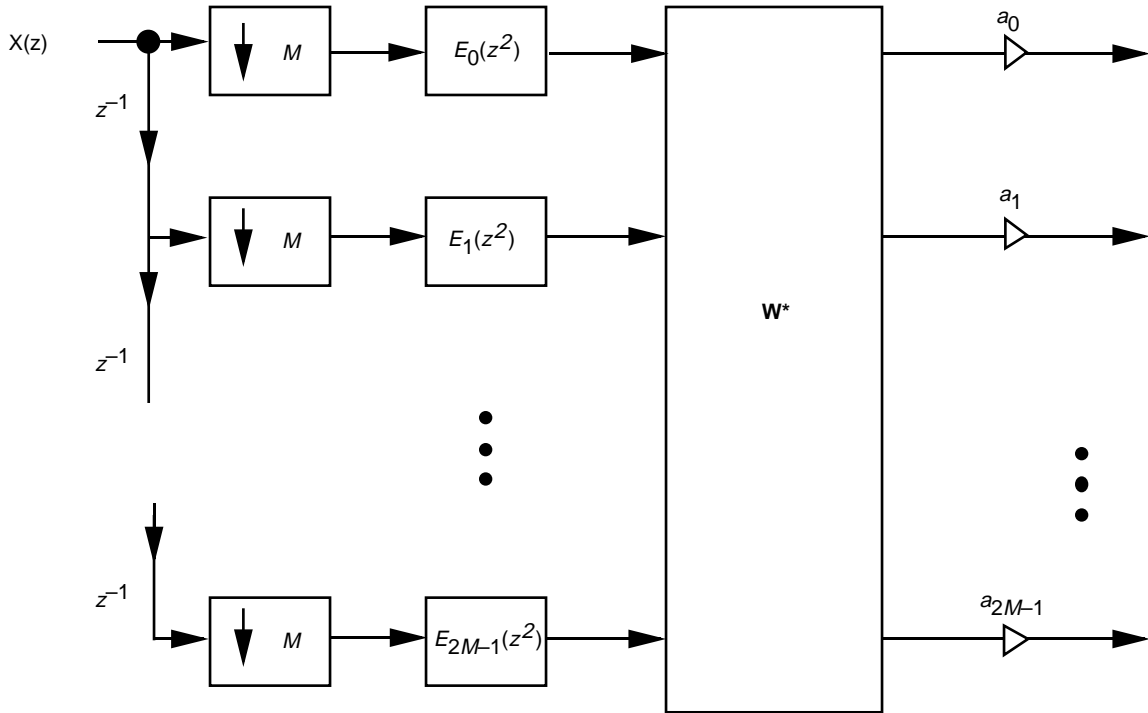

Fig. 6. Efficient implementation of the analysis bank of the 2*M*–channel DFT filter bank. The DFT matrix, W, is of size 2*M* x 2*M*.

III. Cosine Modulated Filter Banks and Application in Tunable Multilevel Filtering

In the DFT filter bank described in the previous section, the analysis and synthesis filters have complex coefficients. If it is desirable for the individual filters to have real coefficients, then we can use the new under-decimated cosine modulated filter bank to be discussed in this section.

The system in Fig. 2 is said to be a cosine modulated filter bank if all analysis and synthesis filters are generated by cosine or sine modulation of one or two prototype filters. In this section, we introduce two classes of new under-decimated cosine modulated filter banks. The systems are nearly alias free. Aliasing error decreases as the stop-band attenuation of the prototype increases. Individual analysis and synthesis filters have real coefficients. We can design the prototypes so that the overall response of the

filter bank is a linear-phase multilevel filter. Furthermore, there exists efficient implementation of this cosine modulated filter bank. The implementation cost of the analysis bank is that of the prototype filter plus two DCT matrices (Appendix). The complexity of an $M \times M$ DCT matrix is only of the order $M \log(M)$ [11]. The same holds true for the synthesis bank. Two types of filter stacking can be applied in the new under-decimated cosine modulated filter bank. In our discussion, a cosine modulated filter bank will be identified as type 1 or type 2 according to the stacking of its analysis and synthesis filters.

A. Type 1 Cosine Modulated Filter Bank

1. Construction of the Type 1 Cosine Modulated Filter Bank. In the cosine modulated filter bank, all analysis and synthesis filters have real coefficients. Each filter has positive and negative spectral occupancy as opposed to single-sided spectral occupancy in the DFT filter bank. This incurs a problem that we do not have in the DFT filter bank. Details and a proposed solution of this new problem will be given below.

Let $P_0(z)$ and $Q_0(z)$ be respectively the prototype filters of the analysis bank and the synthesis bank. The definitions of $P_k(z)$ and $Q_k(z)$ are as in Section II. To get real-coefficient analysis and synthesis filters from the prototypes, we can combine $P_k(z)$ and $P_{-k}(z)$:

$$H_k(z) = a_k P_k(z) + a_k^* P_{-k}(z), \qquad F_k(z) = b_k Q_k(z) + b_k^* Q_{-k}(z), \qquad k = 1, 2, \cdots, M - 1$$

Since $P_0(z)$ and $P_M(z)$ are already real filters, we can directly choose

$$H_k(z) = 2a_k P_k(z), \qquad F_k(z) = 2b_k Q_k(z), \qquad k = 0 \text{ or } M$$

Figure 7 shows the spectral supports of the analysis filters for the type 1 cosine modulated filter bank. The stacking of the spectral supports of the synthesis filters is similar.
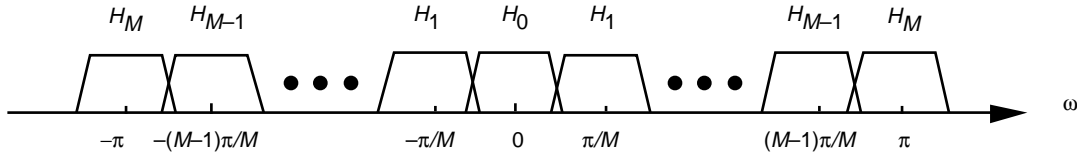

Fig. 7. Normalized magnitude responses of the analysis filters of the type 1 cosine modulated filter bank.

Aliasing error due to M-fold decimation in the 0th and the Mth subband can be suppressed on the synthesis side as we did in the DFT filter bank. The situation in the other subbands is different because now $H_k(z)$ and $F_k(z)$, $k = 1, 2, \cdots, M - 1$, are bandpass filters. Referring to Fig. 8, decimation by M followed by expansion by M in the subbands will cause one image copy of $P_k(z)$ to overlap completely with $Q_{-k}(z)$, $k = 1, 2, \cdots, M - 1$. This type of aliasing error cannot be suppressed in the synthesis bank.

Our solution to this problem is to introduce a second subsystem that has exactly the same aliasing error to cancel the existing one. Let the second subsystem have analysis filters $H_k'(z)$ and synthesis filters $F_k'(z)$, $k = 1, 2, \cdots, M - 1$. To create the same aliasing error, the filters of the second subsystem are required to have similar stacking as that of the first subsystem. In particular,

$$H_k'(z) = a_k' P_k(z) + a_k'^* P_{-k}(z), \quad F_k'(z) = b_k' Q_k(z) + b_k'^* Q_{-k}(z), \quad k = 1, 2, \cdots, M - 1$$

The configuration of the analysis filters in the second subsystem is shown in Fig. 9. Notice that the spectral occupancy of $H_0(z)$ and $H_M(z)$ are not covered in the second subsystem.

(a)

$|P_k(e^{j\omega}W^{-2k-2})|$ $|P_k(e^{j\omega}W^{-2k})|$ $|P_k(e^{j\omega}W^{-2k+2})|$ $|P_k(e^{j\omega}W^{-2})|$ $|P_k(e^{j\omega}W^2)|$

$-(k+2)\pi/M$ $-k\pi/M$ $-(k-2)\pi/M$ 0 $(k-2)\pi/M$ $(k+2)\pi/M$ ω

(b)

FROM Q_{-k}

FROM Q_k

$|F_k(e^{j\omega})|$

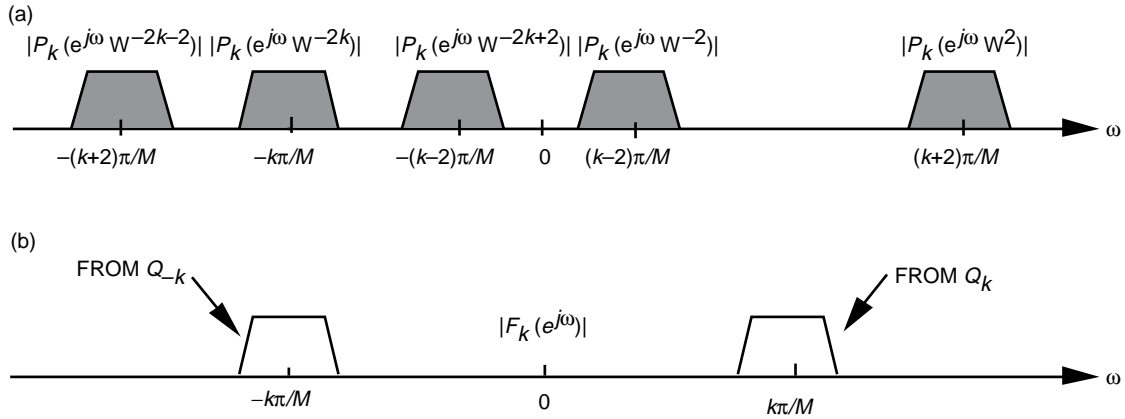$-k\pi/M$ 0 $k\pi/M$ ω

Fig. 8. Type 1 cosine modulated filter bank: (a) image copies of $P_k(z)$ due to decimation followed by expansion and (b) the spectral support of $F_k(z)$.
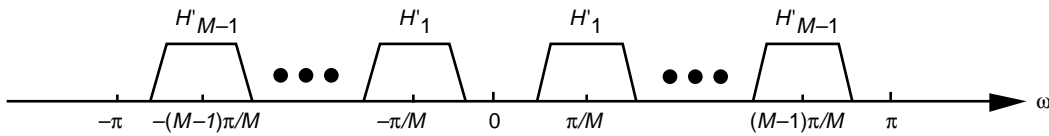

H'_{M-1} H'_1 H'_1 H'_{M-1}

$-\pi$ $-(M-1)\pi/M$ $-\pi/M$ 0 π/M $(M-1)\pi/M$ π ω

Fig. 9. Normalized magnitude responses of the analysis filters of the second subsystem in the type 1 cosine modulated filter bank.

The setup of the new system is now complete and is shown in Fig. 10. It is a connection of two subsystems. The first subsystem has $M + 1$ channels, and the second subsystem has $M - 1$ channels. The whole system is under-decimated; it has $2M$ channels but is decimated only by M. The analysis and synthesis filters can be summarized as follows:
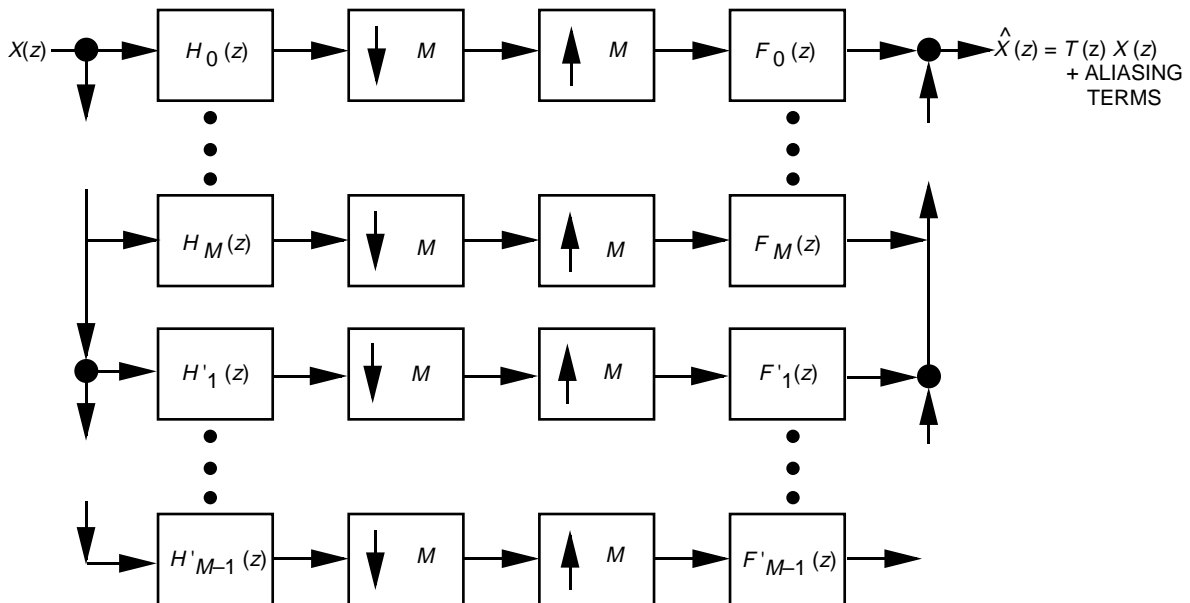

Fig. 10. The setup for the type 1 under-decimated cosine modulated filter bank.

113

$$H_k(z) = 2a_k P_k(z), \qquad\qquad k = 0, M$$

$$H_k(z) = a_k P_k(z) + a_k^* P_{-k}(z), \qquad k = 1, 2, \cdots, M-1$$

$$H'_k(z) = a'_k P_k(z) + a_k'^* P_{-k}(z), \qquad k = 1, 2, \cdots, M-1$$

(12)

$$F_k(z) = 2b_k Q_k(z), \qquad\qquad k = 0, M$$

$$F_k(z) = b_k Q_k(z) + b_k^* Q_{-k}(z), \qquad k = 1, 2, \cdots, M-1$$

$$F'_k(z) = b'_k Q_k(z) + b_k'^* Q_{-k}(z), \qquad k = 1, 2, \cdots, M-1$$

The values of a_k, a'_k, b_k, and b'_k will be determined later.

In the following we show that with proper design of the prototypes and appropriate choices of a_k, a'_k, b_k, and b'_k, this filter bank is almost alias free. The overall response of the type 1 cosine modulated filter bank can be designed to be a linear-phase tunable multilevel filter.

2. Cancellation and Suppression of Aliasing Error. As we mentioned in the construction of filters, the aliasing error in the 0th and the Mth subbands will be *suppressed* in the synthesis bank. Only the subbands with bandpass filters require alias *cancellation*. The physical picture is as follows:

Consider the kth subband, $1 \le k \le M-1$. Due to decimation followed by expansion, $P_k(z)$ has $M-1$ image copies and $P_{-k}(z)$ also has $M-1$ image copies. The image copies of $P_k(z)$ will be suppressed by $Q_k(z)$ provided that both $P_0(z)$ and $Q_0(z)$ have stop-band edges less than π/M and large enough stop-band attenuation. Of the $M-1$ image copies of $P_k(z)$, $M-2$ of them are in the stop band of $Q_{-k}(z)$ and, hence, will be suppressed by $Q_{-k}(z)$, as depicted in Fig. 8. However, one of the image copies of $P_k(z)$ will fall on top of the spectral support of $Q_{-k}(z)$. Only this image copy requires cancellation. In the kth subband of the second subsystem, the same aliasing occurs. It can be shown that the aliasing error of the second subsystem cancels that of the first subsystem if the values of a_k, b_k, a'_k, and b'_k are chosen properly. Mathematical proof of this claim is as follows.

With filters constructed as in Eq. (12) and the expression of alias transfer functions in Eq. (3), we have

$$A_i(z) = \frac{1}{M} \left(A_i^{(1)}(z) + A_i^{(2)}(z) + A_i^{(3)}(z) + A_i^{(4)}(z) \right)$$

(13)

where

$$A_i^{(1)}(z) = (a_0 b_0 + a_0^* b_0) P_0 \left(zW^{2i} \right) Q_0(z) + \sum_{k=1}^{M-1} (a_k b_k + a'_k b'_k) P_k \left(zW^{2i} \right) Q_k(z)$$

$$A_i^{(2)}(z) = \sum_{k=1}^{M-1} (a_k^* b_k + a_k'^* b'_k) P_{-k} \left(zW^{2i} \right) Q_k(z)$$

$$A_i^{(3)}(z) = \sum_{k=1}^{M-1} (a_k b_k^* + a'_k b_k'^*) P_k \left(zW^{2i} \right) Q_{-k}(z)$$

$$A_i^{(4)}(z) = (a_0^* b_0^* + a_0 b_0^*) P_0 \left(zW^{2i}\right) Q_0(z) + \sum_{k=1}^{M-1} (a_k^* b_k^* + a_k'^* b_k'^*) P_{-k} \left(zW^{2i}\right) Q_{-k}(z)$$

Assume $P_0(z)$ and $Q_0(z)$ satisfy Eq. (5). It follows that $A_i^{(1)}(z) \approx 0$ and $A_i^{(4)}(z) \approx 0$. Let $a_k, k = 0, \cdots, M$ be real and choose

$$b_k = a_k, \qquad k = 0, \cdots, M$$

$$a_k' = -ja_k, \quad b_k' = ja_k, \quad k = 1, \cdots, M-1$$

(14)

If a_k, b_k, a_k', and b_k' are chosen as above, it can be verified that $a_k^* b_k + a_k'^* b_k' = 0$, which implies $A_i^{(2)}(z) = A_i^{(3)}(z) = 0$. So the condition $A_i(z) \approx 0$ is ensured, provided that Eq. (5) is valid and a_k, b_k, a_k', and b_k' are chosen according to Eq. (14).

With Eq. (14), we can write down the time domain description of the analysis and synthesis filters for the type 1 cosine modulated filter bank. Let $p_0(n)$ be the impulse response of $P_0(z)$ and $q_0(n)$ be the impulse response of $Q_0(z)$.

$$h_k(n) = 2a_k p_0(n) \cos (kn\pi/M), \qquad k = 0, 1, \cdots, M$$

$$h_k'(z) = 2a_k p_0(n) \sin (kn\pi/M), \qquad k = 1, 2, \cdots, M-1$$

(15)

$$f_k(z) = 2a_k q_0(n) \cos (kn\pi/M), \qquad k = 0, 1, \cdots, M$$

$$f_k'(n) = 2a_k q_0(n) \sin (kn\pi/M), \qquad k = 1, 2, \cdots, M-1$$

From the expression in Eq. (15), we can see that each individual filter is a sine or cosine modulation of the prototype filters.

3. The Magnitude Response of the Overall Response $T(z)$. Using Eqs. (12) and (6), we get

$$T\left(e^{j\omega}\right) = \frac{2}{M} \sum_{k=0}^{M} |a_k|^2 \left(\left(R_0(e^{j(\omega+k\pi/M)}\right) + R_0\left(e^{j(\omega-k\pi/M)}\right)\right)$$

(16)

The above expression for the overall response is similar to that in the case of DFT filter bank, Eq. (7). If $R_0(z)$ is a Nyquist $(2M)$ filter, this is a tunable multilevel filter bank like in a DFT filter bank.

4. The Phase of the Overall Response $T(z)$. The overall response $T(z)$ has linear phase provided that $R_0(z)$ is linear phase and N_r, the order of $R_0(z)$, is an even multiple of M. The reason is given below. The linear phase property of $R_0(z)$ entitles us to write

$$R_0\left(e^{j\omega}\right) = e^{-j\omega N_r/2} R(\omega)$$

(17)

where $R(\omega)$ is a real-valued function. Substitute Eq. (17) into Eq. (16) and we get

$$T\left(e^{j\omega}\right) = \frac{4}{M} e^{-j\omega N_r/2} \sum_{k=0}^{M} |a_k|^2 \left(e^{jk\pi N_r/2M} R\left(\frac{\omega - k\pi}{M}\right) + e^{-jk\pi N_r/2M} R\left(\frac{\omega + k\pi}{M}\right) \right)$$

which has linear phase when N_r is a multiple of $2M$.

Notice that if $Q_0(z)$ is the time reversed version of $P_0(z)$, i.e., $Q_0(z) = z^{-N_p}\widetilde{P_0}(z)$, then $F_k(z)$ and $F_k'(z)$ are the time-reversed version of $H_k(z)$ and $H_k'(z)$, respectively. With this choice of $Q_0(z)$, the overall response is

$$T(z) = \frac{z^{-N_p}}{M} \left(\sum_{k=0}^{M} H_k(z)\widetilde{H_k}(z) + \sum_{k=1}^{M-1} H_k'(z)\widetilde{H_k'}(z) \right)$$

In this case, the overall response has linear phase regardless of the order of $R_0(z)$.

5. The Phase of the Individual Analysis and Synthesis Filters. Let the prototype filter $P_0(z)$ be linear phase. If the center of symmetry of $p_0(n)$ coincides with that of the sine or cosine functions that modulate $p_0(n)$, then the resulting analysis filters also have linear phase. In the case of the type 1 cosine modulated filter bank, the condition can be further reduced. It can be verified that if N_p, the order of $P_0(z)$, is a multiple of M, every analysis filter has linear phase. The same holds for the synthesis bank.

When N_p is an even multiple of M, all the analysis filters in the second subsystem, $H_k'(z), k = 1, 2, \cdots, M - 1$, are found to have a null at zero frequency and π. We can also verify that as N_p is an odd multiple of M, the analysis filters $H_k(e^{j\omega}), k = 1, 2, \cdots, M - 1$, have zeros at zero frequency and π. We conclude that some $M - 1$ of the $2M$ analysis filters have zeros at zero frequency and π if the analysis filters have linear phase. More on this property will be addressed when we present a similar result for the type 2 cosine modulated filter bank.

Summarizing, we have shown that the filter bank in Fig. 10 is equivalent to a linear-phase tunable multilevel filter if the following two conditions hold: (1) The nonadjacent bands of $P_0(z)$ and $Q_0(z)$ do not overlap, [Eq. (5)], and (2) $R_0(z)$ is linear phase and close to a Nyquist $(2M)$ filter. The implementation cost of the analysis bank, as will be shown in the Appendix, is the prototype filter $P_0(z)$ plus two DCT matrices. Complexity follows the buildup of the architecture; the computational cost of the analysis bank is that of $P_0(z)$ plus two DCT matrices working at an M-fold decimated rate.

B. Type 2 Cosine Modulated Filter Bank

In Figs. 7 and 9, we show the configuration of the analysis filter for the type 1 under-decimated cosine modulated filter bank. In the type 2 cosine modulated under-decimated filter bank, a different stacking of filters is applied. We show the new setup in Fig. 11. The filter bank can still be conceived as a connection of two subsystems, both with M channels. The spectral supports of the second set of analysis filters are exactly the same as the spectral supports of the first set of analysis filters (Fig. 12). The same holds for the synthesis bank. To be more specific, let $P_0(z)$ and $Q_0(z)$ be the two prototypes as before. Define

$$\widehat{P}_k(z) = P_0\left(zW^{k+0.5}\right) \qquad \text{and} \qquad \widehat{Q}_k(z) = Q_0\left(zW^{k+0.5}\right), \quad W = e^{-j\pi/M}$$
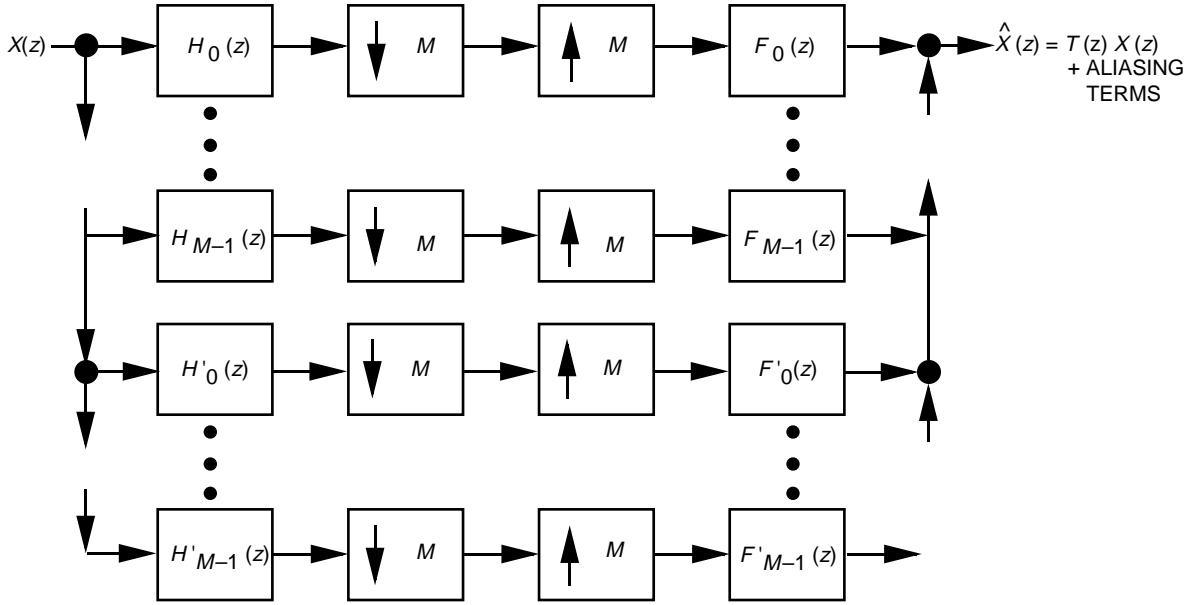
Fig. 11. The setup for the type 2 under-decimated cosine modulated filter bank.
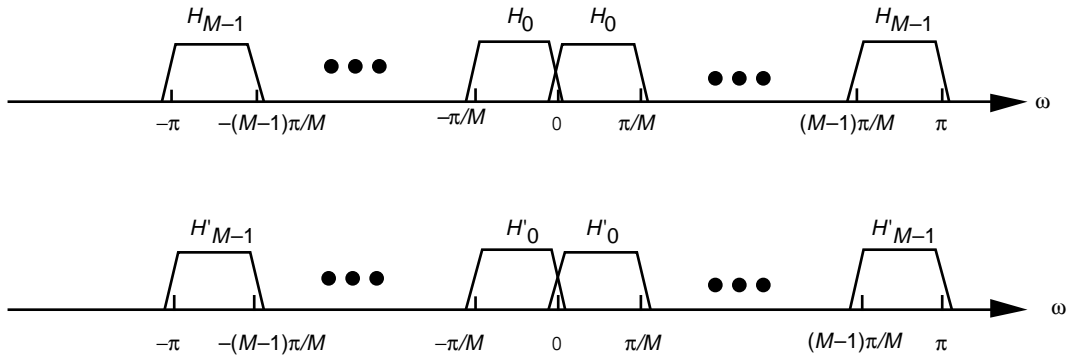

Fig. 12. Normalzed magnitude responses of the analysis filters of the type 2 cosine modulated filter bank.

Spectral support of $\widehat{P}_k(z)$ is shown in Fig. 13. It is similar for $\widehat{Q}_k(z)$. Notice the difference between the definition of $\widehat{P}_k(z)$ and the definition of $P_k(z)$ in the type 1 cosine modulated filter bank, Fig. 3; if the type 1 system and the type 2 system have the same analysis prototype, then there is on the unit circle $P'_k(z)$ a shift of $P_k(z)$ by $\pi/2M$, and this comes from the extra $W^{0.5}$ in the preceding equation.
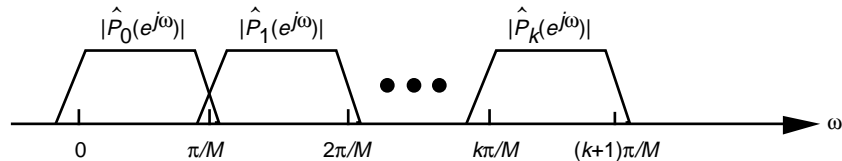

Fig. 13. Magnitude responses of $\hat{P}_k(z)$.

We choose the analysis and synthesis filters, similar to the construction of the type 1 system, as follows:

117

$$H_k(z) = a_k \widehat{P}_k(z) + a_k^* \widehat{P}_{-k}(z), \qquad k = 0, 1, \cdots, M-1$$

$$H_k'(z) = -j\left(a_k \widehat{P}_k(z) - a_k^* \widehat{P}_{-k}(z)\right), \qquad k = 0, 1, \cdots, M-1$$

$$F_k(z) = b_k \widehat{Q}_k(z) + b_k^* \widehat{Q}_{-k}(z), \qquad k = 0, 1, \cdots, M-1 \tag{18}$$

$$F_k'(z) = j\left(b_k \widehat{Q}_k(z) - b_k^* \widehat{Q}_{-k}(z)\right), \qquad k = 0, 1, \cdots, M-1$$

In this case, we found that the overall response is still equivalent to a tunable multilevel filter, and the argument of alias cancellation continues to hold after minor adjustments. More details are given below. The implementation cost and the computational complexity are the same as for the type 1 system. This can be proved in a manner similar to that used for the type 1 system in the Appendix.

1. Cancellation and Suppression of Aliasing Error. The cancellation and suppression of aliasing error is very similar to that of the type 1 cosine modulated filter bank. The image copies of $\widehat{P}_k(z)$, Fig. 14(a), can suppressed by $\widehat{Q}_k(z)$, provided that $P_0(z)$ and $Q_0(z)$ have large enough stop-band attenuation and their nonadjacent bands do not overlap. We can see from Fig. 14(a) that two image copies of $\widehat{P}_k(z)$ overlap with $\widehat{Q}_{-k}(z)$. Figure 14(b) shows the resulting aliasing that cannot be suppressed by the synthesis filters. As in the type 1 case, the second subsystem contributes another alias term, which can be used to cancel the alias from the first subsystem. This can be verified by directly substituting the analysis and synthesis filter in Eq. (18) into the definition of alias transfer functions in Eq. (3).
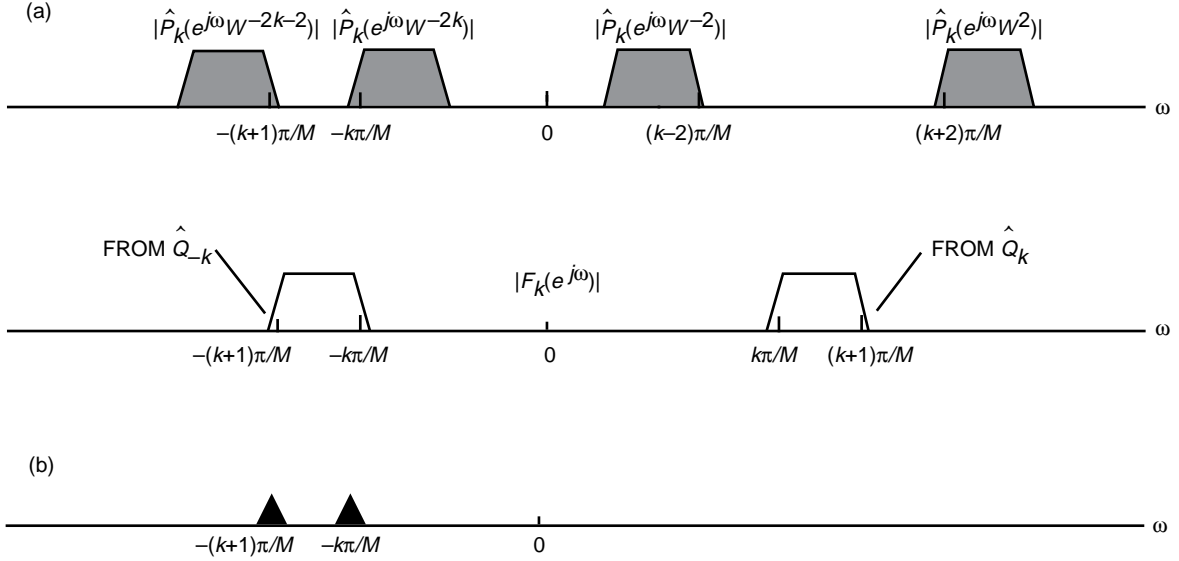

Fig. 14. Type 2 cosine modulated filter bank: (a) image copies of $\widehat{P}_k(z)$ due to decimation followed by expansion and the spectral support of $F_k(z)$ and (b) residual alias component that cannot be suppressed by $\widehat{Q}_k(z)$.

2. The Magnitude Response of the Overall Response $T(z)$. The overall response $T(z)$ in the type 2 cosine modulated filter bank can still be expressed in a form similar to that in the type 1 case. Let $R_0(z)$ be defined as before, that is, $R_0(z) = P_0(z)Q_0(z)$. With analysis and synthesis filters chosen as in Eq. (18), the overall response is

$$T(z) = \frac{2}{M} \sum_{k=-M}^{M-1} |a_k|^2 R_0 \left(e^{j(\omega - \pi(k+0.5)/M)} \right)$$

As in the DFT filter bank, the magnitude response of $T(z)$ will resemble that of a multilevel filter if $R_0(z)$ is a Nyquist $(2M)$ filter or close to a Nyquist $(2M)$ filter. Again, we can tune the values of a_k as desired; the overall response is actually a tunable multilevel filter.

3. The Phase Response of the Overall Response $T(z)$**.** In the type 1 cosine modulated filter bank, the phase of $T(z)$ is linear if $R_0(z)$ is linear phase and N_r, the order of $R_0(z)$, is an even multiple of M. It is still true in the type 2 system. We can verify this by following the same steps as in the type 1 case.

4. The Phase Responses of the Individual Filters. Each analysis filter in the type 1 cosine modulated filter bank has linear phase if $P_0(z)$ has linear phase and N_p, the order of $P_0(z)$, is an even multiple of M. The same holds for the synthesis bank. This is still true in the type 2 case. However, the type 2 system is found to have the following two additional properties when the individual filters are linear-phase:

(i) The filters $H_0'(z)$ and $F_0'(z)$ have zeros at zero frequency, i.e., $H_0'\left(e^{j0}\right) = F_0'\left(e^{j0}\right) = 0$. The highpass filters $H_{M-1}'(z)$ and $F_{M-1}'(z)$ have zeros at π.

(ii) Either $H_0(z)$ or $F_0(z)$ has a bump at zero frequency and either $H_{M-1}(z)$ or $F_{M-1}(z)$ has a bump at π.

Property (i): Let $P_0(z)$ be linear phase and a_0 be real. Referring to the construction of filters in Eq. (18), the impulse responses of $H_k(z)$ and $H_k'(z)$ are, respectively, $h_k(n)$ and $h_k'(n)$:

$$h_k(n) \; = \; 2a_0 p_0(n) \cos\left(\pi(k+0.5)\frac{n}{M}\right)$$

$$h_k'(n) \; = \; 2a_0 p_0(n) \sin\left(\pi(k+0.5)\frac{n}{M}\right)$$

Their time reversed versions are

$$h_k(N_p - n) \; = \; 2a_0 p_0(n) \cos\left(\pi(k+0.5)\frac{n}{M} - \pi(k+0.5)\frac{Nr}{M}\right)$$

$$h_k'(N_p - n) \; = \; -2a_0 p_0(n) \sin\left(\pi(k+0.5)\frac{n}{M} - \pi(k+0.5)\frac{Nr}{M}\right)$$

For the above two filters to have linear phase, N_r is necessarily a multiple of $2M$. If N_r is an even multiple of $2M$, then $h_k(n) = h_k(N_p - n)$ and $h_k'(n) = -h_k'(N_p - n)$. When N_r is an odd multiple of $2M$, $H_k(z)$ becomes odd symmetric and $H_k'(z)$ becomes even symmetric. Without loss generality, we can assume that N_r is an even multiple of $2M$.

Notice that an even N_p, $h_k'(n) = -h_k'(N_p - n)$ implies that $H_k'(e^{j0}) = H_k'(e^{j\pi}) = 0$ [7]. In particular, the lowpass filter $H_0'(z)$ has a notch at zero frequency, and the highpass filter $H_{M-1}'(z)$ has a notch at π.

The other filters, $H'_k(z), k = 1, 2, \cdots, M - 2$, are all bandpass filters; zeros at zero frequency do not have a significant effect on their shapes. The same holds true for the synthesis bank.

In the type 1 cosine modulated filter bank, we obtained similar results. In that case, when the analysis filters have linear phase, some $M - 1$ of them have zeros at zero frequency and π. But those are all bandpass filters; zeros at zero frequency and π are not of particular importance.

Property (ii): For the flatness of the passband of $T(z)$, $R_0(z)$ is required to be a Nyquist $(2M)$ filter or close to a Nyquist $(2M)$ filter, as we have discussed previously. The Nyquist property of $R_0(z)$ ensures that

$$\sum_{k=-M}^{M-1} R\left(e^{j\omega} W^{k+0.5}\right) = c$$

for some constant c. Without loss of generality, we can consider $c = 1$. At zero frequency, only the term $k = -1$ and the term $k = 0$ contribute significantly, so

$$R_0\left(e^{j\pi/2M}\right) + R_0\left(e^{-j\pi/2M}\right) \approx 1 \tag{19}$$

Since $R_0(z)$ is a real filter, we have

$$\left|R_0\left(e^{j\pi/2M}\right)\right| = \left|R_0\left(e^{-j\pi/2M}\right)\right| \tag{20}$$

Combining Eqs. (19) and (20) leads to $\left|R_0\left(e^{j\pi/2M}\right)\right| \geq 0.5$, i.e., $\left|P_0\left(e^{j\pi/2M}\right) Q_0\left(e^{j\pi/2M}\right)\right| \geq 0.5$. This in turn implies $\left|P_0\left(e^{j\pi/2M}\right)\right| \geq \sqrt{0.5}$ or $\left|Q_0\left(e^{j\pi/2M}\right)\right| \geq \sqrt{0.5}$. Suppose $\left|P_0\left(e^{j\pi/2M}\right)\right| \geq \sqrt{0.5}$. Moreover, by the linear phase property of $P_0(z)$, we can write $P_0\left(e^{j\omega}\right) = e^{-j\omega N_p/2} P(\omega)$, where $P(\omega)$ is a real-valued function. With this expression, $H_0\left(e^{j0}\right)$ becomes

$$H_0\left(e^{j0}\right) = e^{-j\omega N_p}\left(e^{jN_p\pi/4M} P\frac{-\pi}{2M} + e^{-jN_p\pi/4M} P\frac{\pi}{2M}\right)$$

From the discussion of property (i), we know N_p is an even multiple of $2M$. This gives us

$$\left|H_0\left(e^{j0}\right)\right| = 2\left|P\frac{\pi}{2M}\right| \geq \sqrt{2}$$

This means that $H_0(z)$ has a bump of about 3 dB at zero frequency. If we assume $\left|Q_0\left(e^{j\pi/2M}\right)\right| \geq \sqrt{0.5}$, then $F_0(z)$ will have a bump of about 3 dB at zero frequency. The filters $H_{M-1}(z)$ and $F_{M-1}(z)$ are shifts of $H_0(z)$ and $F_0(z)$ by π; if either $H_0(z)$ or $F_0(z)$ has a bump at zero frequency, then either $H_{M-1}(z)$ or $F_{M-1}(z)$ has a bump at zero frequency.

In the above derivation, we assume a_k is a real number. The readers will find that for complex a_k, properties (i) and (ii) continue to hold after minor adjustments of the above argument.

It is noteworthy that the null of $H'_0(z)$ and $F'_0(z)$ at zero frequency and the bump of $H_0(z)$ or $F_0(z)$ at zero frequency do not affect the overall response. The overall response is a summation of responses of the first subsystem and the second subsystem. The bump from the first subsystem compensates for the null of the second subsystem to ensure the flatness of the overall response $T(z)$.

IV. Design Procedures

We now discuss four techniques for designing $P_0(z)$ and $Q_0(z)$. The resulting $R_0(z) = P_0(z)Q_0(z)$ is close to a Nyquist $(2M)$ filter and, at the same time, the nonadjacent bands of $P_0(z)$ and $Q_0(z)$ do not overlap, i.e., $P_0(z)$ and $Q_0(z)$ satisfy Eq. (5). The prototypes $P_0(z)$ and $Q_0(z)$ designed by these methods can be applied to both the DFT filter banks and the two classes of cosine modulated filter banks.

A. Eigenfilter Design

The basic idea of this method is the following. Let $P_0(z)$ be a lowpass filter with a stop-band edge less than π/M. (Any lowpass filter design technique can be used for designing $P_0(z)$.) First we find the condition for $Q_0(z)$ such that the product $R_0(z) = P_0(z)Q_0(z)$ is Nyquist $(2M)$. Then we use an eigenfilter design and incorporate this condition to design $Q_0(z)$ [7]. The condition is derived below.

Let N_r, N_p, and N_q be, respectively, the orders of $R_0(z)$, $P_0(z)$, and $Q_0(z)$. Let the impulse responses of $R_0(z)$, $P_0(z)$, and $Q_0(z)$ be $r_0(n)$, $p_0(n)$ and $q_0(n)$, respectively. Then $r_0(n)$ is the convolution of $p_0(n)$ and $q_0(n)$, i.e.,

$$r_0(n) = \sum_{m=0}^{N_q} p_0(n-m)q_0(m) \tag{21}$$

Given $p_0(n)$, we want to constrain $q_0(n)$ so that $r_0(n)$ is a Nyquist $(2M)$ filter. In this case, $q_0(n)$ must satisfy

$$\sum_{m=0}^{N_q} p_0(2Mn-m)q_0(m) = c\delta(n-n_0) \tag{22}$$

for some n_0 and c. Constant c is a scalar factor; we can consider $c = 1$. The equivalent of Eq. (22) in matrix form is

$$\mathbf{r} = \mathbf{P}\mathbf{q} \tag{23}$$

where $\mathbf{r}$ is a $(\lfloor (N_p + N_q)/2M \rfloor + 1) \times 1$ column vector with the n_0th entry equal to 1 and all others equal to 0, $\mathbf{P}$ is a $(\lfloor (N_p + N_q)/2M \rfloor + 1) \times (N_q + 1)$ matrix with

$$[\mathbf{P}]_{mn} = \begin{cases} p_0(2Mm - n + 1), & \text{if } 2Mm - n + 1 \geq 0 \\ 0, & \text{otherwise} \end{cases}$$

and $\mathbf{q} = [q_0(0)\ q_0(1)\ \cdots\ q_0(N_q)]^T$.

The condition in Eq. (23) can be easily incorporated in the eigenfilter approach [7].

B. A Shortcut Design

Let $P_0(z)$ be a Nyquist $(2M)$ lowpass filter with zero phase. Let $Q_0(z)$ also be zero phase with its passband covering $P_0(z)$ as depicted in Fig. 15, i.e., $Q_0(e^{j\omega}) \approx 1$ in the passband and the transition band of $P_0(e^{j\omega})$. Because $R_0(z)$ differs from $P_0(z)$ only in the stop band where the magnitude of $P_0(z)$ is small, we have
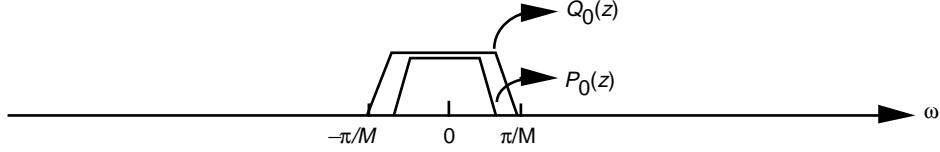
Fig. 15. The passband of $Q_0(z)$ covers the passband and transition band of $P_0(z)$.

$$R_0(z) \approx P_0(z) \tag{24}$$

In this case, $R_0(z)$ will still be close to a Nyquist $(2M)$ lowpass filter.

In the above discussion, $P_0(z)$ and $Q_0(z)$ are zero phase and, hence, noncausal. Some delays can be added to make the filter bank causal, since both prototypes are FIR. In the two following methods, the synthesis prototype $Q_0(z)$ is chosen as the time-reversed version of $P_0(z)$, i.e., $Q_0(z) = z^{-N_p}\widetilde{P}_0(z)$, where N_p is the order of $P_0(z)$.

C. Nonlinear Optimization of $P_0(z)$

The filter coefficients of $P_0(z)$ can be directly optimized to minimize the stop-band energy of $P_0(z)$ subject to the Nyquist condition in Eq. (22). The stop-band energy of $P_0(z)$ is

$$\phi_s = \int_{(\pi/2M)+\epsilon}^{\pi} |P_0\left(e^{j\omega}\right)|^2 d\omega$$

But with $Q_0(z) = z^{-N_p}P_0(z)$, the right-hand side of Eq. (22) becomes a quadratic form of $p_0(n)$. To minimize ϕ_s, we need a nonlinear optimization package that can incorporate nonlinear constraints. The detail of this design technique is documented in [12].

Instead of optimizing the coefficients of $P_0(z)$ with nonlinear constraints, we can use a objective function to reflect how close $R_0(z)$ is to a Nyquist $(2M)$ filter. A possible objective function is

$$\phi_p = \int_0^{\pi/M} \left(|P_0\left(e^{j\omega}\right)|^2 + |P_0\left(e^{j(\omega-(\pi/M))}\right)|^2 - 1\right)^2 d\omega$$

Combining both ϕ_s and ϕ_p, let

$$\phi = \alpha\phi_p + (1-\alpha)\phi_s$$

where $0 < \alpha < 1$. The new objective function ϕ can be minimized using the usual nonlinear optimization programs (e.g., [13]) without any constraints.

D. Kaiser Window Design

In this approach, $P_0(z)$ is a lowpass filter with an even order obtained through Kaiser window design. That is,

$$p_0(n) = \frac{\sin(\omega_c n)}{\pi n}w(n)$$

where $w(n)$ is a Kaiser window [7]. After we choose the stop-band attenuation and the width of the transition band, the length of the window can be estimated by a formula developed by Kaiser. In this case, the window is completely determined [7]. The cutoff frequency ω_c of the ideal filter is the only free parameter left for the design of $P_0(z)$.

According to Eq. (22), we choose a simple objective function, ϕ_{Kaiser}, to reflect the closeness of $R_0(z)$ to a Nyquist $(2M)$ filter:

$$\phi_{Kaiser} = \max_n |r_0(2Mn) - \delta(n - n_0)|$$

Experiments show that ϕ_{Kaiser} is a convex function of ω_c; we can adjust the parameter ω_c to find the best $P_0(z)$, which yields the smallest ϕ_{Kaiser}. Design examples will be given in the next section.

E. Comparison of the Four Design Methods

Of all the four approaches stated above, the shortcut design and the Kaiser window design are probably the easiest. In the shortcut design approach, we only need to design two lowpass filters with certain specifications described above. In the Kaiser window design, only the parameter ω_c needs to be optimized, yet no nonlinear optimization is involved. Also, the value of the objective function ϕ_{Kaiser} at a given ω_c can be computed easily.

V. Design Example

We now present one design example of the under-decimated system. The type 1 cosine modulated filter bank is used in this example. The Kaiser window approach is adopted for the design of the prototype filter.

Example 1: Tunable Multilevel Filter. The system has 20 channels. In this case, $M = 10$. The analysis bank prototype filter $P_0(z)$ is linear phase with order $N_p = 120$, stop-band attenuation 85 dB, passband edge $\omega_p = 0.04\pi$, and stop-band edge $\omega_s = 0.099\pi$. The synthesis bank prototype $Q_0(z)$ is chosen as the time-reversed version of $P_0(z)$. As elaborated in Section III, the resulting overall response will have linear phase. Figure 16(a) shows the magnitude response of $P_0(z)$. The normalized magnitude responses of the analysis filters are shown in Fig. 16(b) and (c). The synthesis filters are time-reversed versions of the analysis filters; the magnitude responses of the synthesis filters are the same as those of analysis filters.

After designing the prototype filters, the values of a_k can be changed freely to obtain the desired overall response, $T(z)$. For instance, we set $a_0 = a_1 = 1$, $a_2 = a_3 = a_4 = 0$, $a_5 = a_6 = a_7 = 0.7$, and $a_8 = a_9 = a_{10} = 0.3$. The magnitude response of the resulting $T(z)$ is plotted in Fig. 16(b). Since $T(z)$ has linear phase, we did not show the phase response. The corresponding dB plot of Fig. 16(d) is shown in Fig. 16(e).
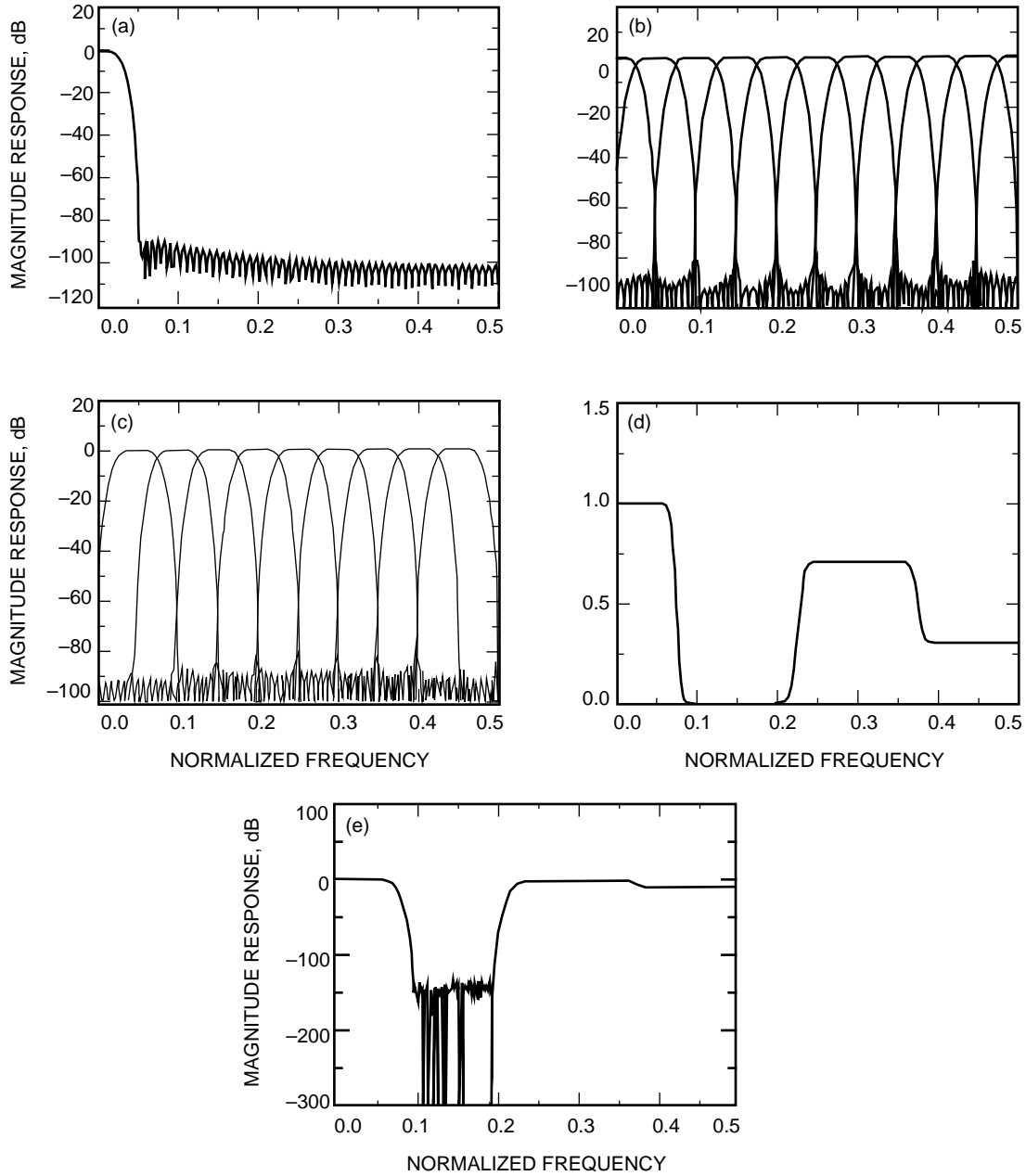
Fig. 16. Example: (a) the magnitude response of the prototype filter, $P_0(z)$, (b) the normalized magnitude responses of the analysis filters in the first subsystem, (c) the normalized magnitude responses of the analysis filters in the second subsystem, (d) the magnitude response of the overall response $T(z)$, and (e) the magnitude response of the overall response $T(z)$ in a dB plot.

References

[1] R. E. Crochiere and L. R. Rabiner, *Multirate Digital Signal Processing*, Englewood Cliffs, New Jersey: Prentice Hall, 1983.

[2] M. J. T. Smith and III. T. P. Barnwell, "A New Filter Bank Theory for Time-Frequency Representation," *IEEE Trans. on Acoustic, Speech and Signal Processing*, vol. ASSP-35, pp. 314–327, March 1987.

[3] M. Vetterli, "A Theory of Multirate Filter Banks," *IEEE Trans. on Acoustic, Speech and Signal Processing*, vol. ASSP-35, pp. 356–372, March 1987.

[4] P. P. Vaidyanathan, "Quadrature Mirror Filter Banks, M-Band Extensions and Perfect Reconstruction Techniques," *IEEE ASSP Magazine*, vol. 4, pp. 420, June 1987.

[5] H. J. Nussbaumer, "Pseudo QMF Filter Bank," *IBM Tech. Disclosure Bulletin,* vol. 24, pp. 3081–3087, November 1981.

[6] J. H. Rothweiler, "Polyphase Quadrature Filters, a New Subband Coding Technique," *Proc. of the IEEE Int. Conf. on Acoustic, Speech and Signal Processing*, pp. 1980–1983, April 1983.

[7] P. P. Vaidyanathan, *Multirate Systems and Filter Banks*, Englewood Cliffs, New Jersey: Prentice Hall, 1993.

[8] P. P. Vaidyanathan, "Orthonormal and Biorthonormal Filter Banks as Convolvers, and Convolutional Coding Gain," *IEEE Tran. on Signal Processing*, vol. SP-41, pp. 2110–2130, June 1993.

[9] C. S. Burrus. "Block Implementation of Digital Filters," *IEEE Trans. on Circuit Theory*, vol. CT-18, pp. 697–701, November 1971.

[10] M. Vetterli, "Running FIR and IIR Filtering Using Multirate Filter Banks," *IEEE Trans. on Acoustic, Speech and Signal Processing*, vol. ASSP-36, pp. 730–738, May 1988.

[11] P. Yip and K. R. Rao, "Fast Discrete Transforms," *Handbook of Digital Signal Processing,* edited by D. F. Elliott, San Diego, California: Academic Press, 1987.

[12] T. Nguyan., "Near-Perfect-Reconstruction Pseudo-QMF Banks," *IEEE Tran. on Signal Processing*, vol. SP 41, pp. 2110–2130, December 1993.

[13] W. H. Press, B. P. Flannery, S. A. Teukolsky, and W. T. Vetterling, *Numerical Recipes,* Cambridge: Cambridge University Press, 1989.

[14] Y.-P. Lin and P. P. Vaidyanathan, "Linear Phase Cosine Modulated Maximally Decimated Filter Banks With Perfect Reconstruction," Technical Report, California Institute of Technology, Pasadena, California, November 1993.

Appendix

Implementation of the Type 1 Cosine Modulated Filter Bank

In this appendix, we prove that the implementation cost of the analysis bank of the type 1 cosine modulated filter bank is that of the analysis prototype filter plus two DCT matrices.

Let

$$P_0(z) = \sum_{n=0}^{2M-1} G_n\left(z^{2M}\right) z^{-n}$$

where $G_n(z)$ is the nth type 1 polyphase component of $P_0(z)$. Then

$$P_k(z) = \sum_{n=0}^{2M-1} G_n\left(z^{2M}\right) z^{-n} W^{-kn} \tag{A-1}$$

Rewriting analysis filters in Eq. (13) in terms of the polyphase components of $P_0(z)$ with a_k, b_k, a'_k, and b'_k as in Eq. (15), we obtain

$$H_k(z) = 2 \sum_{n=0}^{2M-1} a_k G_n\left(z^{2M}\right) z^{-n} \cos\left(\frac{\pi}{M}kn\right), \qquad k = 0, 1, \cdots, M$$

$$H'_k(z) = 2 \sum_{n=0}^{2M-1} a_k G_n\left(z^{2M}\right) z^{-n} \sin\left(\frac{\pi}{M}kn\right), \quad k = 1, 2, \cdots, M-1 \tag{A-2}$$

Define a $2M$-component vector $\mathbf{h}(z)$ given by

$$\mathbf{h}(z) = \begin{pmatrix} H_0(z) \\ \vdots \\ H_M(z) \\ H'_1(z) \\ \vdots \\ H'_{M-1}(z) \end{pmatrix}$$

Using Eq. (A-2), $\mathbf{h}(z)$ can be written as

$$\mathbf{h}(z) = 2 \begin{pmatrix} \mathbf{A}_0 & \mathbf{0} \\ \mathbf{0} & \mathbf{A}_1 \end{pmatrix} \begin{pmatrix} \mathbf{C} & \Lambda_0 \mathbf{C} \\ \mathbf{S} & \Lambda_1 \mathbf{S} \end{pmatrix} \begin{pmatrix} \mathbf{g}_0(z^{2M}) & \mathbf{0} \\ \mathbf{0} & \mathbf{g}_1(z^{2M}) \end{pmatrix} \begin{pmatrix} \mathbf{e}(z) \\ z^{-M}\mathbf{e}(z) \end{pmatrix} \tag{A-3}$$

where $\mathbf{g}_i(z)$, Λ_i, and $\mathbf{A}_i$ are diagonal matrices with

$$[\mathbf{g}_0(z)]_{kk} = G_k(z), \quad [\mathbf{g}_1(z)]_{kk} = G_{k+M}(z), \quad k = 0, 1, \cdots, M-1 \tag{A-4}$$

$$[\Lambda_0]_{kk} = (-1)^k, \quad k = 0, 1, \cdots, M$$

$$[\Lambda_1]_{kk} = (-1)^k, \quad k = 1, 2, \cdots, M-1 \tag{A-5}$$

$$[\mathbf{A}_0]_{kk} = a_k, \quad k = 0, 1, \cdots, M$$

$$[\mathbf{A}_1]_{kk} = a_k, \quad k = 1, 2, \cdots, M-1 \tag{A-6}$$

and $\mathbf{C}$ and $\mathbf{S}$ are $(M+1) \times M$ and $(M-1) \times M$ matrices with

$$[\mathbf{C}]_{mn} = \cos(\frac{\pi}{M}mn), \quad m = 0, \cdots, M, \quad n = 0, \cdots, M-1$$

$$[\mathbf{S}]_{mn} = \sin(\frac{\pi}{M}mn), \quad m = 1, \cdots, M-1, \quad n = 0, \cdots, M-1 \qquad \text{(A-7)}$$

Define two $M \times 2M$ matrices

$$\mathbf{T}_0 = (\mathbf{C} \quad \Lambda_0\mathbf{C}) \qquad \text{and} \qquad \mathbf{T}_1 = (\mathbf{S} \quad \Lambda_1\mathbf{S})$$

From Eq. (A-3), we can draw Fig. A-1, a schematic implementation of the $2M$ channel cosine modulated system. The input to $\mathbf{T}_0$ and $\mathbf{T}_1$, $\mathbf{a}(n)$, can be partitioned into two $M \times 1$ vectors:

$$\mathbf{a}(n) = \begin{pmatrix} \mathbf{a}_0(n) \\ \mathbf{a}_1(n) \end{pmatrix}$$

Their dependence on n will be dropped for convenience. As indicated in Fig. A-1, $\mathbf{d}_0$ and $\mathbf{d}_1$ are the outputs of $\mathbf{T}_0$ and $\mathbf{T}_1$, respectively:

$$\mathbf{d}_0 = \mathbf{T}_0\mathbf{a} \qquad \text{and} \qquad \mathbf{d}_1 = \mathbf{T}_1\mathbf{a}$$

From the definitions of $\mathbf{T}_0$ and $\mathbf{T}_1$, we know

$$\mathbf{d}_0 = \mathbf{C}\mathbf{a}_0 + \Lambda_0\mathbf{C}\mathbf{a}_1 \qquad \text{and} \qquad \mathbf{d}_1 = \mathbf{S}\mathbf{a}_0 + \Lambda_1\mathbf{S}\mathbf{a}_1 \qquad \text{(A-8)}$$

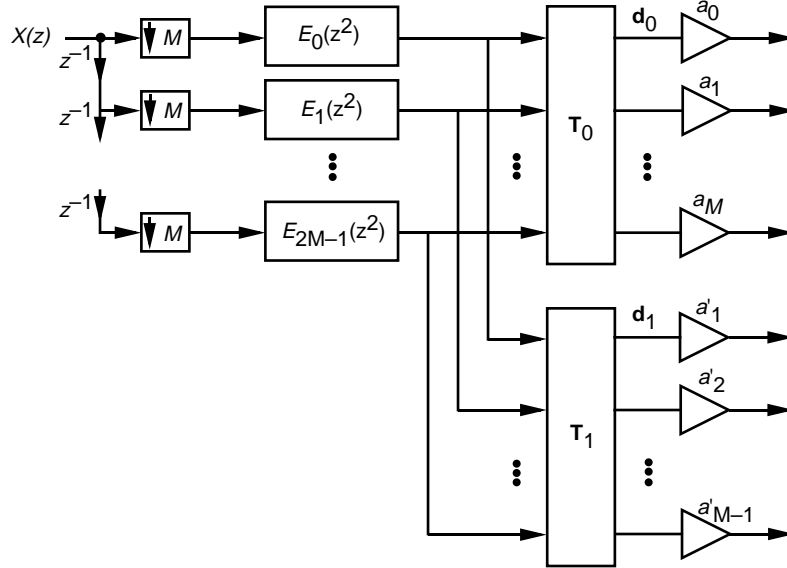In [14], it is pointed out that $\mathbf{C}$ and $\mathbf{S}$ have the following properties:

Fig. A-1. A schematic for the implementation of the analysis bank of the type 1 under-decimated cosine modulated 2*M*-channel filter bank.

$$\mathbf{\Lambda}_0 \mathbf{C} = \mathbf{C} \begin{pmatrix} 0 & \mathbf{0} \\ \mathbf{0} & \mathbf{J}_{M-1} \end{pmatrix} + \mathbf{r} \begin{pmatrix} 1 & 0 & \cdots & 0 \end{pmatrix} \qquad \text{and} \qquad \mathbf{\Lambda}_1 \mathbf{S} = -\mathbf{S} \begin{pmatrix} 0 & \mathbf{0} \\ \mathbf{0} & \mathbf{J}_{M-1} \end{pmatrix}$$

Using these relations, Eq. (A-8) becomes

$$\mathbf{d}_0 = \mathbf{C} \left(\mathbf{a}_0 + \begin{pmatrix} 0 & \mathbf{0} \\ \mathbf{0} & \mathbf{J}_{M-1} \end{pmatrix} \mathbf{a}_1 \right) + [\mathbf{a}_1]_0 \, \mathbf{r}, \quad \mathbf{d}_1 = \mathbf{S} \left(\mathbf{a}_0 - \begin{pmatrix} 0 & \mathbf{0} \\ \mathbf{0} & \mathbf{J}_{M-1} \end{pmatrix} \mathbf{a}_1 \right) \qquad \text{(A-9)}$$

where $[\mathbf{a}_1]_0$ is the first element of $\mathbf{a}_1$, and $\mathbf{r} = [1 \ -1 \ \cdots \ (-1)^{M-1}]^T$. Equation (A-9) allows us to have a more clear idea of the implementation of $\mathbf{T}_0$ and $\mathbf{T}_1$. The implementation of the synthesis bank is similar to the above.

Now we can draw a more detailed and complete picture for the implementation of the $2M$ channel filter bank. For simplicity, we can choose the synthesis filters to be the time-reversed versions of the corresponding analysis filters without the scalars a_k. The efficient implementation of the filter bank is shown in Fig. A-2. From Fig. A-2, we can see that the major complexity of the analysis bank is the cost of the analysis prototype plus matrix $\mathbf{C}$ and matrix $\mathbf{S}$. Matrices $\mathbf{C}$ and $\mathbf{S}$ can be implemented by fast algorithms for DCT and DST matrices [11]. The process is similar for the synthesis bank.

SIZE OF MATRICES:

$\mathbf{g}_0 (z^2)$, $\mathbf{g}_1 (z^2)$ $M \times M$

$\mathbf{C}$ $(M+1) \times M$

$\mathbf{S}$ $(M-1) \times M$
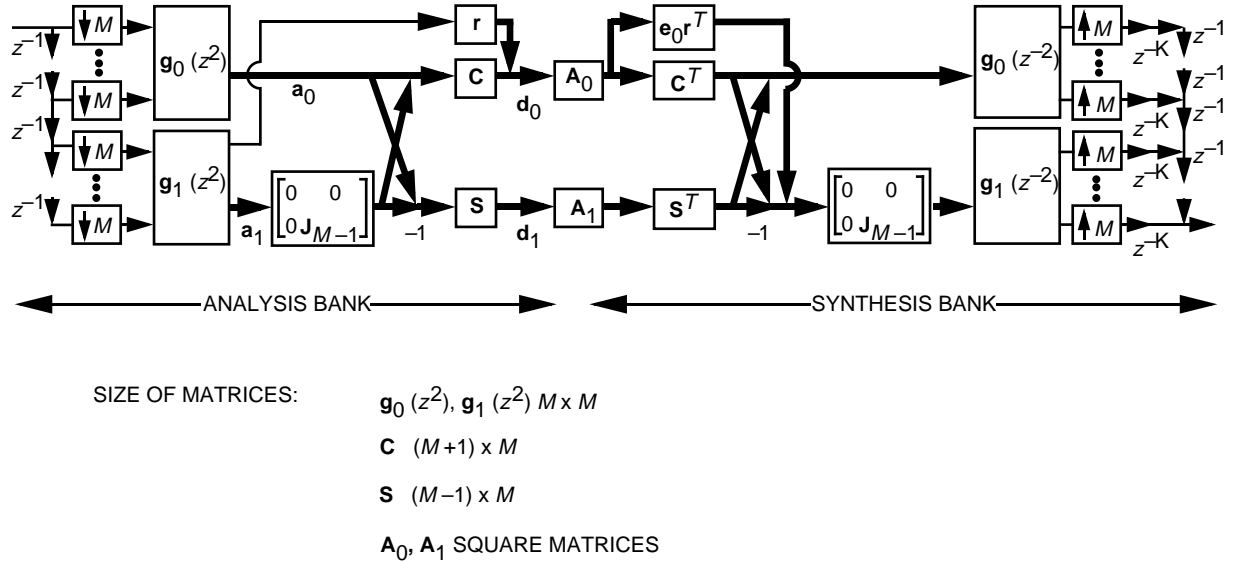
$\mathbf{A}_0$, $\mathbf{A}_1$ SQUARE MATRICES

Fig. A-2. Efficient implementation of the type 1 under-decimated cosine modulated 2M-channel filter bank, where $k = N - 2M + 1$ and $\mathbf{e}_0 = [1 \, 0 \ldots 0]^T$.